This is a relation which gives $|F_H|^2$ in terms of $|F_m|^2$ and $|F_P|^2$. The positive and negative signs before the second term in equation (11) correspond respectively to the negative and positive values of $\cos\alpha$. In most cases, α is acute and hence only the negative sign before the second term need be considered (*cf.* the approximation made in the paragraph following equation (3), Kartha & Parthasarathy, 1965).

In practice, to a good approximation $1/k^2$ may be neglected as compared with unity. Then equation (11) reduces to

$$|F_H|^2=|F_m|^2+|F_P|^2-2[|F_m|^2|F_P|^2-(k/4)^2(\Delta I)^2]^{\frac{1}{2}} . \quad (12)$$

Equation (11) is exact but equation (12) may be used without introducing much error ($<3\%$) due to the approximation $1/k^2 \ll 1$.

The scale factor

In the derivation of equations (11) and (12) it is assumed that the two sets of data $|F_P|$ and $|F_{HP}|$ are on a common scale. (The absolute scales are not necessary for this method). It is well known that the Wilson's method of obtaining average intensity and hence the method of scaling (Wilson, 1942) is not valid in the case of proteins (Harker, 1953). By using the following method, accurate relative scale factors may be determined.

If the scale factors of $|F_P|$ and $|F_{HP}|$ be S_P and S_{HP}, then equations (7) and (9) can be rewritten in the form

$$|F_H|=\frac{k(\Delta I)S_{HP}^2}{4S_P|F_P|\sin\varphi} \quad (13)$$

and

$$S_{HP}^2|F_m|^2=S_P^2|F_P|^2+(1+1/k^2)|F_H|^2 +2|F_P||F_H|S_P\cos\varphi . \quad (14)$$

Eliminating $|F_H|$ from equation (14) with the help of (13) and neglecting $1/k^2$ in comparison with 1 gives

$$S_{HP}^2S_P^2|F_m|^2|F_P|^2\sin^2\varphi=S_P^4|F_P|^4\sin^2\varphi +(k/4)^2(\Delta I)^2S_{HP}^4+(k/4)(\Delta I)S_{HP}^2|F_P|^2S_P^2\sin 2\varphi=0 . \quad (15)$$

If the average is taken over a large number of reflexions $\overline{\sin^2\varphi}=\frac{1}{2}$ and $\overline{\sin 2\varphi}=0$. Thus equation (15) reduces to

$$S_R^4\overline{|F_P|^4}-S_R^2\overline{|F_m|^2|F_P|^2}+(k^2/8)\overline{(\Delta I)^2}=0 , \quad (16)$$

where $S_R^2=S_P^2/S_{HP}^2$. As k varies with $\sin\theta$ the reflexions may be divided in small intervals of $\sin\theta$ such that k does not vary appreciably in the interval chosen. The scale factor is given by

$$S_R^2=[\overline{|F_m|^2|F_P|^2}+\{\overline{|F_m|^2|F_P|^2}^2 -(k^2/2)\overline{(\Delta I)^2}\ \overline{|F_P|^4}\}^{1/2} .]/2\overline{|F_P|^4} .$$

It must be noted that the method does not need the knowledge of the total number of the heavy atoms in the unit cell.

The authors wish to thank Professor Dorothy Hodgkin and Mrs Eleanor Coller for some discussions and Dr B.W. Matthews of the Medical Research Council, Cambridge, for kindly providing a preprint of his paper.

References

HARDING, M. M. (1962). D. Phil. Thesis, Oxford Univ.
HARKER, D. (1953). *Acta Cryst.* **6**, 731.
KARTHA, G. & PARTHASARATHY, R. (1965). *Acta Cryst.* **18**, 745.
MATTHEWS, B. W. (1965). *Acta Cryst.* **20**, 320.
WILSON, A. J. C. (1942). *Nature, Lond.* **150**, 152.

Acta Cryst. (1966). **21**, 280

The crystal structure of $[Cr(H_2O)_4Cl_2]Cl \cdot 2H_2O$.*

By B. MOROSIN, *Sandia Laboratory, Albuquerque, New Mexico, U.S.A.*

(*Received* 2 *February* 1966 *and in revised form* 2 *March* 1966)

We here compare the almost identical results of two independent three-dimensional crystal structure studies of $[Cr(H_2O)_4Cl_2]Cl \cdot 2H_2O$, and present several supplementary illustrations. The duplication of effort was discovered only when one study was almost complete (Morosin, 1965) and the other had recently been accepted for publication (Dance & Freeman, 1965).

Experimental

Single crystals (plates bound by {111}, {1$\bar{1}$1} and well developed {001}) suitable for X-ray studies were obtained by recrystallization of the commercially available salt. Weissenberg and precession photographs were used to determine the symmetry of the compound and the perfection of the specimen used for intensity measurements. Systematic absences and final agreement between observed and calculated structure factors indicate $C2/c$ to be the correct space group. Lattice constants (Table 1)† were obtained with Cu $K\alpha$ radiation ($\lambda K\alpha_1=1{\cdot}54050$ Å) by least-squares fit of 44 high 2θ values measured from films on which lead nitrate powder patterns ($a_0=7{\cdot}8404$ Å) were superimposed. Three-dimensional Mo $K\alpha$ intensity data were collected with the use of balanced filters and a scintillation counter. Angles were set by a semi-automatic or 'remote' control Datex module. Small absorption corrections ($\mu=19{\cdot}0$ cm^{-1}) were calculated with a modified ORABS program (Wehe, Busing & Levy, 1962) and applied for the plate of approximate dimensions $0{\cdot}6\times0{\cdot}6\times0{\cdot}15$ mm. A Patterson synthesis yielded Cr and Cl positions; subsequent Fourier synthesis indicated probable oxygen positions. Positional and thermal parameters

Table 1. *Lattice constants*

	Dance & Freeman	This work
a_0	12·053 (±2)	12·055 (±1)
b_0	6·840 (±2)	6·832 (±1)
c_0	11·640 (±2)	11·648 (±1)
β	94·169 (±5)	94·143 (±8)
V	957·0 Å^3	956·85 Å^3
D_x	1·849 g.cm^{-3}	1·849 g.cm^{-3}
D_m*	1·835 g.cm^{-3}	Dm 1·845 g.cm^{-3}

* Value of Biltz & Birk (1925).

* This work was supported by the U.S. Atomic Energy Commission.

† Throughout this note in Tables and Figures, the value of the error corresponds to the least significant digits in the function value.

Table 2. *Observed and calculated structure factors*

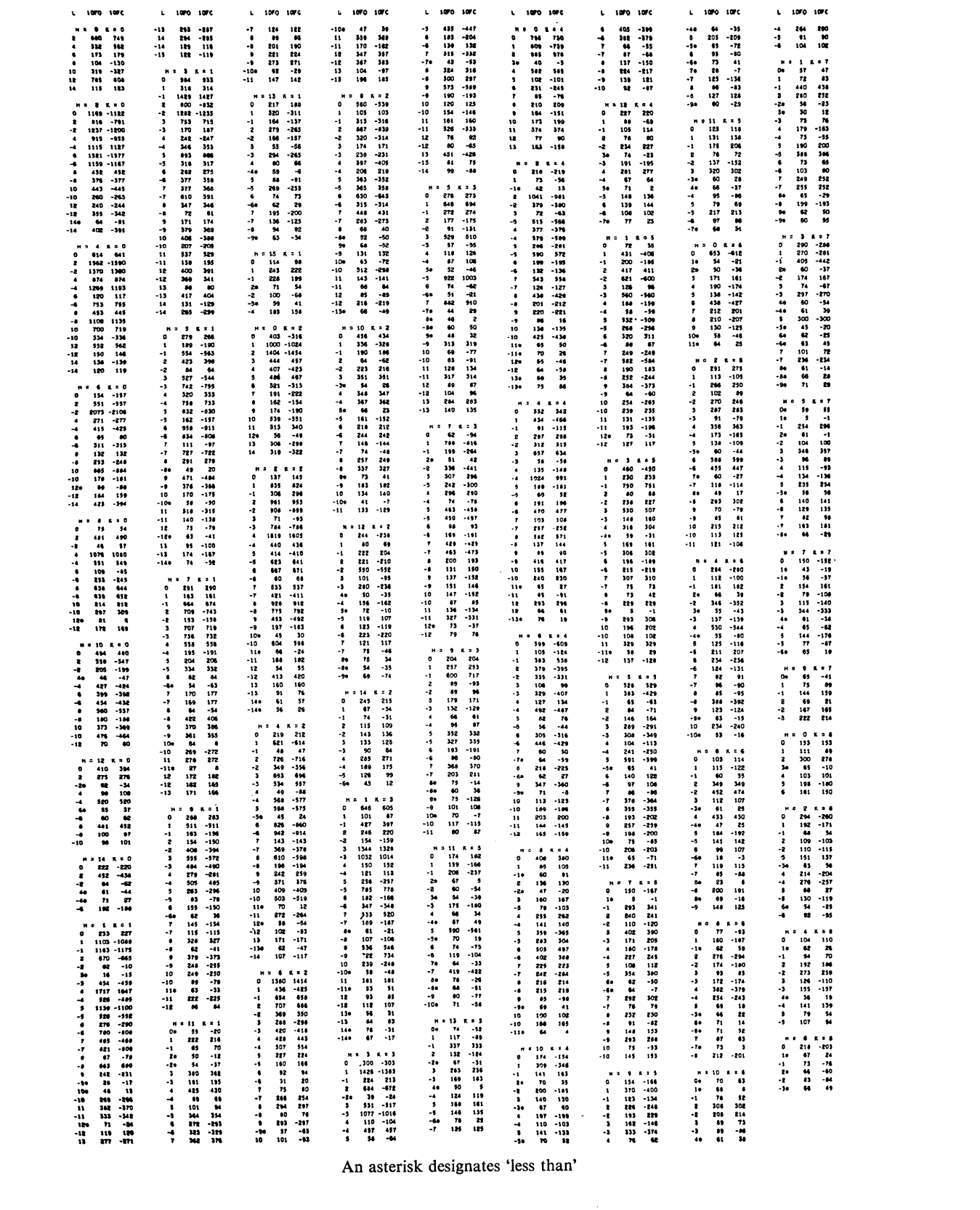

An asterisk designates 'less than'

were refined by the least-squares method (modified ORFLS; Stewart & High, 1964; Busing, Martin & Levy, 1962) with the function, $\Sigma w(F_o - F_c)^2$, minimized. Initially, unit weights were assigned to all observed reflections. Final refinement cycles with anisotropic temperature factors used weights* as a function of F_{meas}, obtained in a manner similar to that of Abrahams & Reddy (1965) with the addition of zero weights assigned to unobserved and the 002 and 020 reflections. Scattering factors used were those of Thomas & Umeda (1957) for Cr^{2+} ion and of Berghuis, Haanappel, Potters, Loopstra, MacGillavry & Veenendaal (1955) for the Cl^- ion and the O atom. Dispersion corrections (*International Tables for X-ray Crystallography*, 1962) for the chromium and chlorine atoms were applied by the method of Templeton (1955). Most computations were carried out on a CDC 3600 computer with a modified 'X-ray 63' system (Stewart & High, 1964; Morosin, 1964).

Structure and comparison of results

The structure factors from the final refinement cycle are given in Table 2. The weighted and unweighted discrepancy indices are 0·046 and 0·041, respectively, for these data (907 observed and 185 unobserved independent reflections) and may be compared with the corresponding values of 0·096 and 0·081, respectively, (listed data consists of 1290 observed and 118 unobserved visually estimated reflections) obtained by Dance & Freeman. The final positional and anisotropic thermal parameters are compared in Tables 3 and 4. The largest difference ($\sim 4\sigma$)† in positional parameters occurs with the y coordinate of Cl(2). However, when the additional positional error arising from the thermal factor is considered, none of the positional parameters may be considered significantly different.

The anisotropic thermal parameters (Table 4) are generally larger in this refinement than those values obtained by Dance & Freeman. This suggests a different $\sin\theta$ dependence between the two sets of data. Small differences in scattering factors [D & F's refinement used Freeman & Watson's (1961) values for chromium and Dawson's (1960) for chlorine], the removal of harmonic contributions by balanced filters (Young, 1965) or different impurity concentrations in the crystals may be partially responsible. The ratios of B_{ii} for chromium, chlorine and oxygen are 2·04, 1·69 and 1·60, respectively. Should the 1·60 ratio be applied to values for different oxygen factors (where similar scattering factors were used), only B_{11} for O(1) and B_{33} for (O3) exceed 1σ. Hence, both sets of anisotropic thermal factors yield the same direction and similar magnitudes as far as the principal axes of the vibration ellipsoids are concerned.

The structure (Fig. 1) consists of three entities (the coordinated chromium ions, chloride ions and water molecules) which are linked together by a network of hydrogen bonds. Each of the water molecules coordinated to the chromium ion forms a hydrogen bond to the chloride ion and to the water molecule. In addition, the chloride ion and the water molecule participate in a slightly longer

Table 3. *Fractional atomic coordinates*

	$x(\sigma_x)$	$y(\sigma_y)$	$z(\sigma_z)$
Cr	0·25	0·25	0·0
Cl(1)	0·0	0·05524 (13)* 0·05530 (30)	0·25
Cl(2)	0·31219 (5) 0·31241 (12)	0·09236 (10) 0·09139 (23)	0·16546 (4) 0·16545 (11)
O(1)	0·39721 (13) 0·39677 (30)	0·19711 (24) 0·19494 (65)	−0·06526 (13) −0·06423 (33)
O(2)	0·30359 (13) 0·30266 (33)	0·50818 (23) 0·50821 (62)	0·06358 (12) 0·06459 (32)
O(3)	0·58737 (13) 0·58692 (34)	0·24803 (29) 0·24894 (66)	0·06968 (12) 0·06947 (37)

* Standard deviations (σ_i) refer to the least significant digits in the function value. The z coordinates are translated $-\frac{1}{2}$ from values listed by Dance & Freeman. Top values are results of this refinement.

Table 4. *Anisotropic thermal parameters*

Thermal parameters are of the form

$$\exp\left(-\tfrac{1}{4}\sum_{i=1}^{3}\sum_{j=1}^{3} B_{ij}h_ih_ja_i^*a_j^*\right)$$

	B_{11}	B_{22}	B_{33}
Cr	2·223 (17) 0·963 (32)	2·149 (18) 1·121 (47)	1·584 (15) 0·837 (32)
Cl(1)	3·017 (30) 1·397 (55)	3·584 (36) 2·069 (79)	2·076 (25) 1·390 (47)
Cl(2)	3·852 (25) 2·305 (47)	3·598 (27) 2·313 (63)	2·191 (18) 1·382 (39)
O(1)	2·663 (59) 1·216 (110)	3·473 (79) 2·242 (174)	2·751 (58) 1·595 (118)
O(2)	3·021 (59) 1·982 (134)	2·705 (63) 1·769 (166)	2·507 (58) 1·413 (118)
O(3)	3·300 (60) 2·013 (142)	3·092 (65) 2·124 (182)	2·925 (59) 2·171 (142)

	B_{12}	B_{13}	B_{23}
Cr	−0·237 (17) −0·110 (16)	−0·349 (12) −0·020 (12)	0·103 (15) 0·083 (16)
Cl(1)	—	−0·159 (21) 0·071 (20)	—
Cl(2)	−0·265 (21) −0·103 (20)	−0·650 (16) 0·178 (16)	0·594 (17) 0·300 (20)
O(1)	0·317 (55) −0·059 (55)	−0·048 (46) 0·114 (47)	0·186 (51) 0·091 (59)
O(2)	−0·225 (54) −0·284 (59)	−0·550 (46) −0·146 (51)	0·037 (50) −0·063 (55)
O(3)	−0·070 (67) 0·004 (67)	−0·016 (46) 0·008 (55)	0·088 (60) 0·075 (67)

* Weights were obtained using standard deviations for F_{meas} of the form:

$$\sigma\langle F_{meas}\rangle = (\sigma^2\langle F^2\rangle + V\langle F^2\rangle)^{\frac{1}{2}}/2F_{meas},$$

where $\sigma^2\langle F^2\rangle$ represents random errors and was calculated from counting statistics and $V\langle F^2\rangle$ attempts to account for systematic errors and was estimated from variation of 'standard' reflections monitored for crystal and alignment stability. The resulting standard deviation of an observation of unit weight, $[\Sigma w(\Delta F)^2/(m-n)]^{\frac{1}{2}}$, where m and n are the number of observations and variables respectively, is 1·24 and would be interpreted to indicate the average value of these weights to be somewhat overestimated. A parallel refinement using unit weights resulted in 12 of 13 positional parameters and 26 of 34 anisotropic thermal parameters within $3\sigma_{tw}$ (tw means 'this work') of values in Tables 3 and 4, the largest departures being $4\sigma_{tw}$ and $6\sigma_{tw}$, respectively.

† $\sigma = (\sigma^2_{tw} = \sigma^2_{\text{Dance and Freeman}})^{\frac{1}{2}}$.

(3·197 Å) interaction. The departure from D_{4h} symmetry of the coordinated chromium ion is small as can be seen by separations given in Fig. 2.

An interesting feature of this structure concerns the relative position of the one remaining hydrogen atom of the water molecule. The nonhydrogenic environment of this particular water molecule is a somewhat distorted trigonal prism (Fig. 3) and geometrical considerations suggest that the remaining hydrogen lies along the pseudo threefold axis formed by the three equal 'a' angles (resulting in a tetrahedrally disposed set of hydrogen linkages about the oxygen). However, in order to retain 105–110° H–O–H angles for the water molecules, the hydrogen positions lie off the lines connecting the heavy atoms as is common in metal halide hydrates. In an attempt to locate these hydrogen positions, a difference synthesis was calculated. Qualitative parameter positions (Table 5) were selected on the basis of the proposed hydrogen network; however, ripple of the same magnitude as the hydrogen peak could be found elsewhere on the map, primarily next to the chromium and chlorine positions. The procedure suggested by Ibers & Cromer (1958) of selecting a maximum $\sin\theta$ value which maximizes the hydrogen peaks while maintaining a minimum value or a shifting position for ripple did not appear

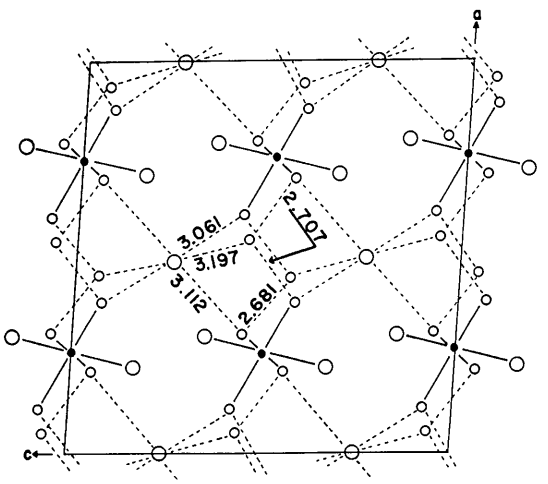

Fig. 1. Crystal structure of $[Cr(H_2O)_4Cl_2]Cl \cdot 2H_2O$ viewed along the b axis. The smaller and larger circles represent oxygen and chlorine atoms respectively. The atoms which are octahedrally coordinated to the chromium atom (small solid circle) are connected by solid lines. The hydrogen bond network is shown by dashed lines and accounts for 5 of 6 independent hydrogen positions. The standard deviation of the separation given is 0·003 Å.

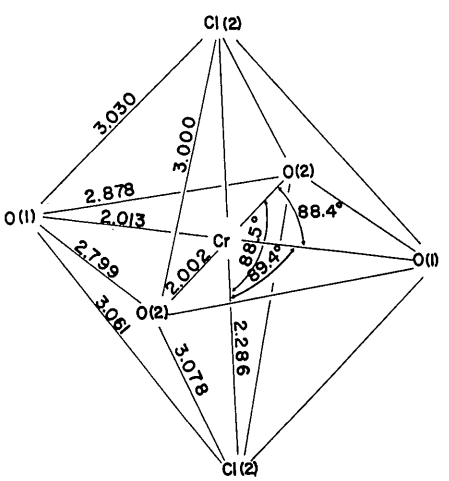

Fig. 2. Octahedral coordination about the chromium ion. The deviation of the complex ion from D_{4h} symmetry is small. The metal ion is situated at a center of inversion. The standard deviation of Cr–Cl, Cr–O, Cl–O and O–O separation 0·001, 0·003, 0·003 and 0·004 Å, respectively, and of metal–ligand angles is 0·2°.

Table 5. *Hydrogen positional parameters*

		x	y	z
O(1)	H(1)	0·09	0·25	0·14
	H(2)	0·03	0·32	0·03
O(2)	H(3)	0·37	0·51	0·11
	H(4)	0·32	0·61	0·01
O(3)	H(5)	0·42	0·31	0·37
	H(6)	0·36	0·16	0·42

Table 6. *Interatomic separations and angles involving hydrogen atoms*

O(1)–H(1)	0·96 Å	H(1)–O(1)–H(2)	100°
O(1)–H(2)	0·95	H(3)–O(2)–H(4)	104
O(2)–H(3)	0·93	H(5)–O(3)–H(6)	110
O(2)–H(4)			
O(3)–H(5)	0·83	O(1)–H(1)–Cl(1)	151
O(3)–H(6)	0·88	O(1)–H(2)–O(3)	153
	0·96	O(2)–H(3)–Cl(1)	165
H(1)–Cl(1)	2·21	O(2)–H(4)–O(3)	153
H(2)–O(3)	1·79	O(3)–H(5)–Cl(1)	155
H(3)–Cl(1)	2·18	O(3)–H(6)–O(2)	160
H(4)–O(3)	1·82	O(3)–H(6)–O(1)	122
H(5)–Cl(1)	2·42	O(3)–H(6)–Cl(2)	110
H(6)–O(2)	2·25		
H(6)–O(1)	2·49		
H(6)–Cl(2)	3·02		

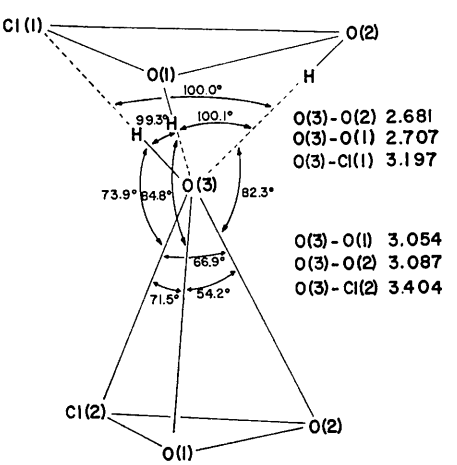

Fig. 3. Nearest neighbor environment about the non-coordinated water molecule. The chlorine and oxygen atoms form a somewhat distorted trigonal prism. The three, near 100° 'a' angles (σ=0·3°), as well as other acute angles shown, suggest that the OH vector lies along the pseudo threefold axis. Interatomic separations involving O(3) and members of the upper triangle (top set of distances) are typical of hydrogen bond separations while those involving atoms of the lower triangle (lower set) are shorter than typical values for van der Waal contact separations.

to give any improvement. Bond angles and separations resulting from these hydrogen positions are found in Table 6. Attempts to grow a crystal large enough for a neutron diffraction study have so far failed.

References

ABRAHAMS, S. C. & REDDY, J. M. (1965). *J. Chem. Phys.* **43**, 2533.

BERGHUIS, J., HAANAPPEL, IJ. M., POTTERS, M., LOOPSTRA, B. O., MACGILLAVRY, C. H. & VEENENDAAL, A. L. (1955). *Acta Cryst.* **8**, 478.

BILTZ, W. & BIRK, E. (1925). *Z. anorg. Chem.* **150**, 20.

BUSING, W. R., MARTIN, K. O. & LEVY, H. A. (1962). ORNL-TM-305, Oak Ridge, National Laboratory Oak Ridge, Tennessee.

DANCE, I. G. & FREEMAN, H. C. (1965). *J. Inorg. Chem.* **4**, 1555.

DAWSON, B. (1960). *Acta Cryst.* **13**, 403.

FREEMAN, A. J. & WATSON, R. E. (1961). *Acta Cryst.* **14**, 231.

IBERS, J. A. & CROMER, D. T. (1958). *Acta Cryst.* **11**, 794.

International Tables for X-ray Crystallography (1962). Vol. III, p.213. Birmingham: Kynoch Press.

MOROSIN, B. (1964). Unpublished.

MOROSIN, B. (1965). Program and Abstracts, Amer. Cryst. Assoc. Meeting, Gatlinburg, Tennessee; paper B-4.

STEWART, J. M. & HIGH, D. F. (1964). Program and Abstracts, Amer. Cryst. Assoc. Meeting, Bozeman, Montana; paper B-13.

TEMPLETON, D. H. (1955). *Acta Cryst.* **8**, 842.

THOMAS, L. H. & UMEDA, K. (1957). *J. Chem. Phys.* **26**, 293.

WEHE, D. J., BUSING, W. R. & LEVY, H. A. (1962). ORNL-TM-229, Oak Ridge National Laboratory, Oak Ridge, Tennessee.

Acta Cryst. (1966). **21**, 284

X-ray diffraction topographs of an elastically distorted crystal.

By YOSHINORI ANDO and NORIO KATO, *Department of Applied Physics, Faculty of Engineering, Nagoya University, Nagoya, Japan*

(*Received* 24 *December* 1965)

Dynamical diffraction phenomena of X-rays are very important for understanding lattice distortion in nearly perfect crystals. This preliminary report concerns the diffraction topographs observed in an elastically distorted crystal of silicon.

The original specimen was nearly free from dislocations, oxygen bands and other lattice distortions. The form of the specimen was a circular disk 8 mm in diameter and 1·4 mm thick. The disk surfaces were parallel to the ($\bar{1}11$) plane. A diametrical compression was applied to the crystal, as shown schematically in Fig. 1. The method of applying the force was similar to that used in the X-ray topograph work of Fukushima, Hayakawa & Nimura (1962, 1963). However, the positional resolution of the present topograph patterns was highly increased by the use of Lang's (1959) technique. Moreover, section-type topographs were also studied (Kato & Lang, 1959). The topographs obtained by Lang's technique are called the traverse patterns, hereafter. The X-ray radiation was $A_gK\alpha_1$.

In Fig. 2 a traverse pattern of the 220 reflexion is shown, the net plane here being perpendicular to the applied force. The diffraction condition is also illustrated in Fig. 2(*b*). *P* indicates the position at which the force was applied to the crystal. The total force was measured by a strain gauge and was a few kilograms in this case. Here, the following points are noticeable:

(*a*) Fringe patterns are recognized in a wide region (*F*) far from the point *P*.

(*b*) Close to *P*, there is a circular region (*E*) which has a very strong reflecting power.

(*c*) In the neighbourhood of the region *E*, a region (*G*) of fairly strong intensity spreads upwards and downwards.

(*d*) On the left side of the region *E*, between *E* and *F*, there is a region (*D*) which reflects X-rays strongly. Precisely speaking, the region *D* overlaps the region *F* to some extent.*

(*e*) If the reflecting condition is reversed, namely the $\bar{2}\bar{2}0$ reflexion is used, the reflecting power of the region *D* becomes less than that of the perfect crystal (departure from Friedel's law).

(*f*) On the other hand, the observations (*a*), (*b*) and (*c*) are not changed essentially when the reflexion condition is reversed.

(*g*) When the force applied at *P* is decreased, the regions *D*, *E*, *F* and *G* contract towards *P*. Even when the wedge *W* contacts the crystal with a force less than 100 grams, a tiny dark spot still remains near *P*, with very faint fringes.

The crystal, upon release from the force, shows the pattern of a perfect crystal, so that all the phenomena described above are caused by elastic distortion. The phenomena (*d*) and (*e*) have already been observed by Fukushima *et al.*

In order to understand the diffraction phenomena in more detail, the section topographs were studied with a very narrow flat pencil of X-rays. A few examples are given in Fig. 3. Positions at which the section topographs were taken are indicated by the arrows in Fig. 2. The magnitude of the

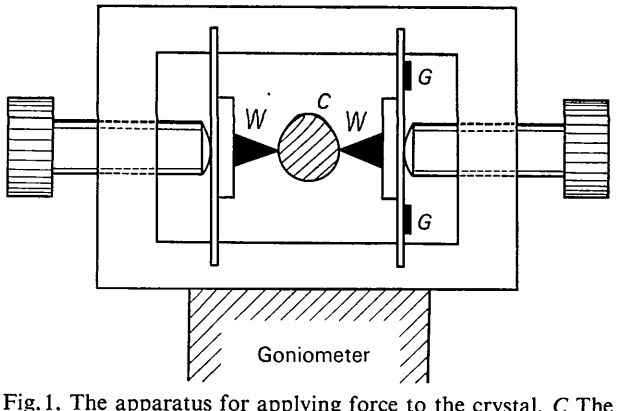

Fig. 1. The apparatus for applying force to the crystal. *C* The specimen. *W* The wedge-shaped block. *G* The elements of the strain gauge.

* In the present case, the force is applied in a slightly asymmetrical way with respect to the net plane.